FACTA UNIVERSITATIS (NIŠ)
SER.: ELEC. ENERG. vol. 15, No. 1, April 2002, 61-71

Development of a Novel Humidity Sensor with Error-Compensated Measurement System

Khalil Arshak, Karen Twomey and Donal Heffernan

Abstract: This paper documents the creation of a complete PC-Based humidity sensing system, implemented using Lab-VIEW from National Instruments. A novel humidity sensor has been manufactured by thin film technology from a combination of In_2O_3/SiO. Both the humidity sensor and a standard temperature sensor are interfaced to a PC using a front-end signal conditioning circuit. The entire system has been analyzed mathematically and the necessary algorithms for error-compensation have been developed. The resulting measurement system is efficient, accurate and flexible.

Keywords: Measurement system, PC based system, humidity sensor, temperature sensor, error compensation, thin film technology.

1 Introduction

Humidity is possibly one of the most difficult environmental parameters to measure [1]. Temperature is a very significant interfering physical variable, which must be eliminated, using appropriate compensation techniques, to ensure an accurate measurement. Dependent on the type of signal conditioning circuit used, there may be additional errors e.g. offset voltage that may also need to be compensated for. A software approach has been adapted in this work to provide the necessary error-corrections.

Manuscript received March 16, 2002. An earlier version of this paper was presented at the 23rd International Conference on Microelectronics, MIEL 2002, May 12-15, 2002, Niš, Serbia.

The authors are with Microelectronics and Semiconductor Research Group, ECE Department, National Technological Park, University of Limerick, Limerick, Ireland (e-mail: khalil.arshak@ul.ie).

2 Sensor Description

The humidity sensor has been produced from a novel combination of indium oxide (In2O3) and silicon monoxide (SiO). There have been a number of different ratios and different vacuum pressures tested. The ratios tried are summarized in Table 1. In this paper the sensors produced at a low pressure of 7×10^{-5} mbar, with a measured thickness of 2000 Å, are discussed (LP#1-4).

Table 1. The different sensor samples produced.

Sensor sample	Materials ratio (%wt.)
LP#1	95%In_2O_3/5%SiO
LP#2	85%In_2O_3/15%SiO
LP#3	75%In_2O_3/25%SiO
LP#4	55%In_2O_3/45%SiO

The thin film structures are prepared using thermal deposition under high vacuum in an Edwards E306A coating unit. The coating unit is equipped with a 550-Watt rotary pump and an E040 diffusion pump capable of achieving a vacuum of 6.5×10^{-7} mbar with the assistance of liquid nitrogen trap facilities. The conductor, with a final thickness of 2000 Åis deposited in an interdigitated pattern at a deposition rate of 20 Å/s. The purpose of this pattern is to increase the admittance of any materials deposited between the interdigits [2]. Next, the sensing layer, of thickness 2000 Å, is deposited in a rectangular pattern over the conductor at a deposition rate of 12 Å/s.

3 Temperature Sensitivity

The effect of temperature on the samples has been investigated. Overall, the samples show a resistance decrease with increasing temperature (Figure 1), as in accordance with the relationship,

$$R = R_0 e^{\frac{E_a}{kT}}$$

where R is the resistance, R_0 is the initial resistance, E_a is the activation energy and k is Boltzmann's constant.

The temperature response can be given in terms of the relative variation, ΔR, of the sensor resistance to a given temperature,

$$\Delta R = \frac{R_0 - R_t}{R_0} \times 100\%$$

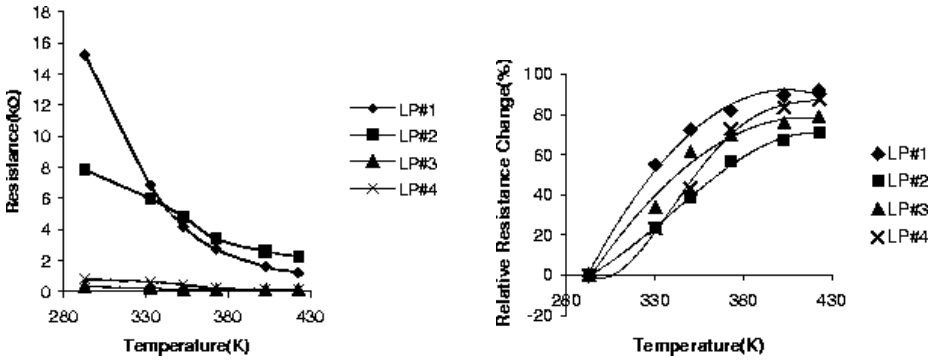

(a) (b)

Fig. 1. (a) Effect of increasing temperature on the resistance of the In_2O_3/SiO samples and (b) The relative resistance change, expressed as a precentage, against increasing temperature for the In_2O_3/SiO.

where R_0 is the initial resistance of the sensor and R_t is the resistance at different temperatures. The calibration curves for the samples were obtained by plotting ΔR against the temperatures, see Figure 1(b). The sensitivity of the samples to the temperatures was determined from the slope of ΔR. The results are shown in Table 2.

Table 2. The temperature sensitivity of the sensor samples.

Sample	Sensitivity(% K)
LP#1	0.8
LP#2	0.5
LP#3	0.6
LP#4	0.8

4 Humidity Sensitivity

The humidity testing of the sensor was conducted using a dynamic humidity chamber. The humidity was ramped from 30RH% to 95RH% in steps of 5RH%. Figure 2 show that the resistance of the samples decreases as the RH% increases. The humidity sensitivity is calculated from the slope of,

$$\frac{R_0 - R_{hum}}{R_0} \tag{1}$$

where R_0 is the initial resistance and R_{hum} is the resistance at increasing humidity levels. The plot of $\Delta R/R_0$ versus increasing relative humidity

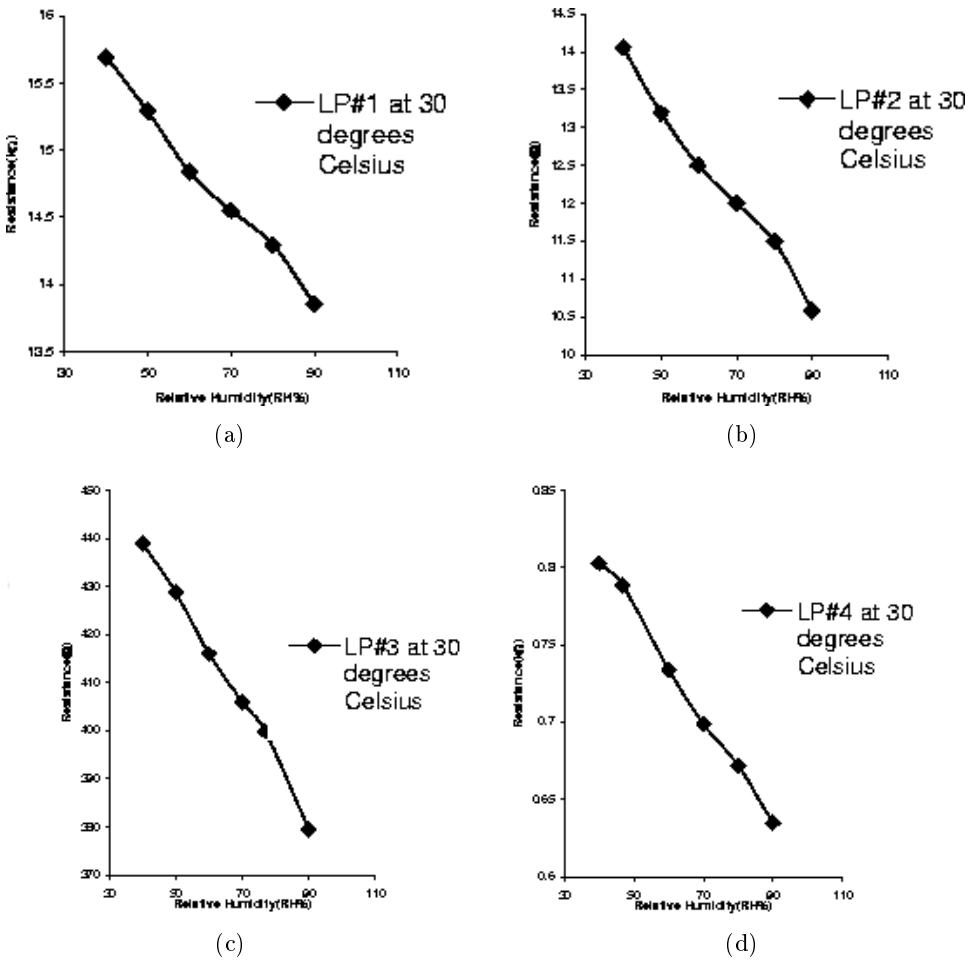

Fig. 2. Effect of increasing humidity on the resistance of the In_2O_3/SiO samples.

levels is shown in Figure 3. All the sensor samples exhibit a resistance decrease with increasing RH%. The response signals have a good linearity for the given RH% range. It has been reported that conduction in thin films occurs through ionic carriers, while electronic conduction at low RH% is negligible [3]. In addition the electrical response will depend on the number of water molecules adsorbed on the sensor surface, as seen in spinel thin film humidity sensors [3]. The absence of capillary pores makes water condensation, and hence electrolytic conduction, impossible. The physically adsorbed multi-layered water molecules on the surface of the thin sensing film play a dominating role for the humidity sensing mechanism [4]. This results in a thin film humidity sensor having a lower humidity sensitivity

than a thick film humidity sensor. However, the advantages to thin films are shorter response time, and a smaller temperature coefficient, due to the lack of condensed water in the pores and the large intrinsic resistance [4].

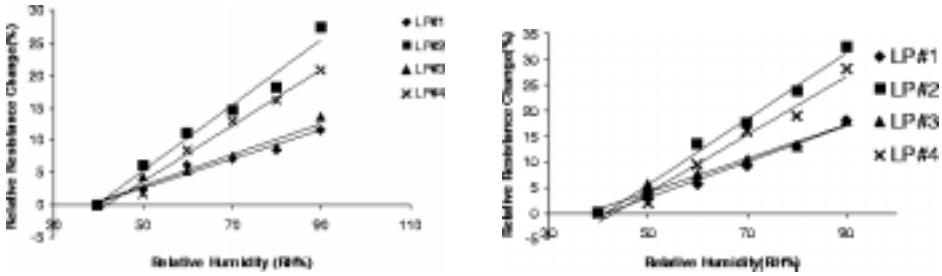

(a) (b)

Fig. 3. (a) The relative resistance change, expressed as a precentage, against increasing humidity for the In_2O_3/SiO samples at 30°C and (b) the relative resistance change, expressed as a precentage, against increasing humidity for the In_2O_3/SiO samples at 60°C.

The following Table 3, lists the humidity sensitivity of each sample at 30 and 60°C. The highest sensitivity is exhibited by LP#2, indicating that the ratio 85%In_2O_3/15%SiO has the greatest potential for use in a humidity sensing application.

Table 3. Relative humidity (%) sensitivity of the sensor samples, at 30°C and 60°C.

Sample	RH% sensitivity at 30°C	RH% sensitivity at 60°C
LP#1	0.222%/RH%	0.352%/RH%
LP#2	0.506%/RH%	0.644%/RH%
LP#3	0.239%/RH%	0.328%/RH%
LP#4	0.436%/RH%	0.566%/RH%

5 Front-End Signal Conditioning

The entire PC-based sensing system is shown in Figure 4. The humidity sensor forms one of the arms of a Wheatstone bridge arrangement, see Figure 5. The output is amplified using an instrumentation amplifier (AD620) so that it will fall in the range of the ADC. The signal is then filtered, using a low pass filter with a cut-off frequency of 10 Hz, to eliminate any high frequency effects. The filter is realized using an opamp, OP07. The sensor signals are connected through an I/O connector, CB-68LP, to a data acquisition card, PCI-MIO-16E-4, that slots into the PC. NI-DAQ data acquisition software runs on this card.

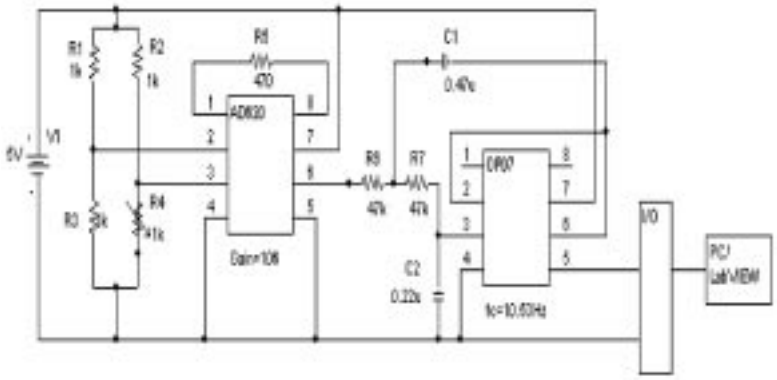

Fig. 4. The PC based sensing system with front-end signal conditioning circuitry.

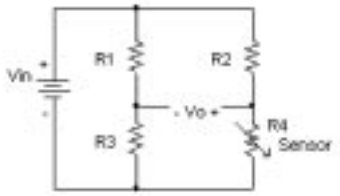

Fig. 5. The Wheatstone Bridge arrangement.

6 System Equation

In general, the Wheatstone Bridge arrangement in Figure 7 can be expressed as,

$$V_o = \frac{R_4}{R_2 + R_4} V_{in} - \frac{R_3}{R_1 + D_3} V_{in} \tag{2}$$

An output voltage ΔV_o develops when the resistors R_1, R_2, R_3 and R_4 are varied by ΔR_1, ΔR_2, ΔR_3 and ΔR_4, respectively. Eqn. (2) can now be rewritten as,

$$\Delta V_o = V_{in} \frac{(R_1 + \Delta R_1)(R_4 + \Delta R_4) - (R_2 + \Delta R_2)(R_3 + \Delta R_3)}{(R_2 + \Delta R_2 + R_4 + \Delta R_4)(R_1 + \Delta R_1 + R_3 + \Delta R_3)} \tag{3}$$

Insertion of typical values into Eqn. (3) and expansion leads to the conclusion that the term $(R_1 + \Delta R_3)(R_2 + \Delta R_4)$ can largely be ignored (¡0.1% of the overall term). ΔV_o can then be rewritten as,

$$\frac{\Delta V_o}{V_{in}} = \frac{R_2 R_4}{(R_2 + R_4)^2} \Big(\frac{\Delta R_1}{R_1} - \frac{\Delta R_2}{R_2} - \frac{\Delta R_3}{R_3} + \frac{\Delta R_4}{R_4} \Big) \tag{4}$$

The humidity sensor forms one of the arms of the Wheatstone bridge. Theoretically, when humidity is sensed the resistance variation is due to R_4 only. Hence,

$$\Delta V_o = V_{in} \frac{R_2 R_4}{(R_2 + R_4)^2} \frac{\Delta R_4}{R_4} \tag{5}$$

This equation is dependent on R_1, R_2 and R_3 having fixed resistor values. In practice, however, ΔV_o may also include variation due to temperature. The temperature is measured from a commercial temperature sensor [5] and the thermal effect of the bridge circuit is then calculated and compensated for. It must also be ensured that the bridge doesn't exhibit any off-null conditions. A common cause of this error is resistance mismatches due to different resistor tolerances. This compensation often involves the use of nulling circuitry, [6], which has the disadvantage of increasing the overall circuit size. In this work, the offnull condition is compensated for using a correction factor based on the resistor tolerances. Therefore, the two main compensation requirements are temperature and offset voltage elimination.

6.1 Temperature compensation

In order to eliminate the effect of temperature on the output voltage readings of the bridge, this effect must be calculated. From Eqn. (5) the resistance change is due to both temperature and humidity effects,

$$\frac{\delta R_4}{R_4} = \left.\frac{\Delta R_4}{R_4}\right|_{\Delta RH} + \left.\frac{\Delta R_4}{R_4}\right|_{\Delta T} \tag{6}$$

The resistance of a resistor at a temperature t is given by [7],

$$R_t = R_0(1 + \alpha t) \tag{7}$$

where R_t is the resistance at t°C, R_0 at 0°C and α is the temperature coefficient of resistance. From Eqn. (7) the change in resistance of R_4 due to temperature is,

$$\left.\Delta R_4\right|_{\Delta T} = R_4 \alpha_{R_4} \Delta T \tag{8}$$

From Eqn. (8),

$$\left.\frac{\Delta R_4}{R_4}\right|_{\Delta T} = \alpha_{R_4} \Delta T \tag{9}$$

Therefore,

$$\left.\frac{\Delta V_o}{V_{in}}\right|_{\Delta T} = \frac{R_2 R_4}{(R_2 + R_4)^2}\alpha_{R_4}\Delta T \tag{10}$$

The change in temperature ΔT is recorded from a temperature circuit utilizing the commercial temperature sensor. α_{R_4} has been calculated from experimental tests to be $-5.4 \times 10^{-3}/^{\circ}$C.

6.2 Offset compensation

The offset voltage is calculated from the tolerances of the resistors. The offset voltage can be expressed as

$$V_{off} = V_{in}\frac{R_1 R_4 - R_2 R_3}{(R_2 + R_4)(R_1 + R_3)} \tag{11}$$

Eqn. (11) can be rewritten as

$$V_{off} = V_{in}\frac{T_1 R\ T_4 R - T_2 R\ T_3 R}{(T_2 R + T_4 R)(T_1 R + T_3 R)} \tag{12}$$

where T_1 represents the tolerance of R_1 and so on for R_2 to R_4. The tolerance T_1 is calculated as follows

$$T_1 = 1 + \frac{\text{Percentage tolerance of} R_1}{100} \tag{13}$$

Simplifying Eqn. (12) gives

$$V_{off} = V_{in}\frac{T_1 T_4 - T_2 T_3}{(T_2 + T_4)(T_1 + T_3)} \tag{14}$$

The effect of off-null conditions on the output voltage can now be isolated.

6.3 Correction factor

The relationship between the bridge output voltage and the applied humidity concentration has been determined from experimental evidence, see Figure 6,

$$\text{RH}\% = \frac{\Delta V_o - 1.3257}{0.0007} \tag{15}$$

ΔV_o was obtained using equations (5) and (14) at increasing humidity concentrations. The predicted RH% is then determined from these values using Eqn. (15).

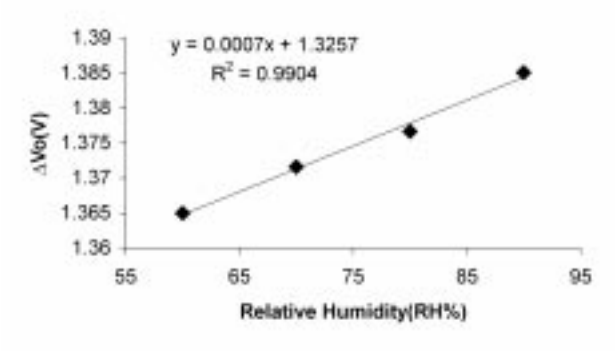

Fig. 6. ΔV_o versus RH%.

Table 4 shows the predicted and applied RH% values. A *multiplying correction factor*, M, has been determined based on the ratio of the predicted RH% to the applied RH%. If the predicted RH% is multiplied by the correction factor the error will be reduced. The correction factor can be modeled by a polynomial equation. Alternatively, an average value of M, 1.03, can be used in place of the complex calculation.

Table 4. The predicted and corrected values of RH%.

Applied RH(%)	Predicted RH(%)	% error in Predicted RH	Corrected RH(%)	% error in corrected RH (%)
60	56.143	6.428333	59.999	0.00166
70	65.629	6.2442857	70.0	0
80	72.29	9.6375	80.0	0
90	84.827	5.74777	90.0	0

7 System Implementation

The data processing and error compensations achieved using Lab-VIEW 6i, are now discussed. The flow diagram of the system overview is shown in Figure 7. In general, on the rising edge of a digital trigger the input channels are sampled. A relatively slow sampling rate of 50 samples per second is chosen due to the slow-changing nature of the sensor signals. The samples are then temporarily stored and the necessary calculations are performed. Figure 8 illustrates the Lab-VIEW block diagram of the error-correction algorithms. Finally, the option exists to store the data for further processing and/or to display the data.

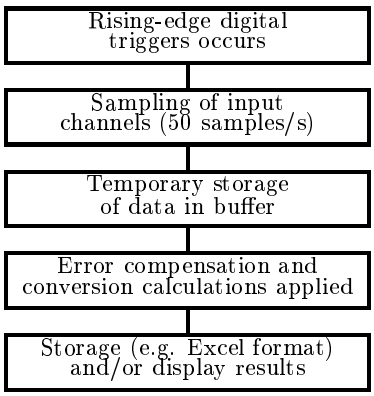

Fig. 7. Layout of Lab-VIEW system.

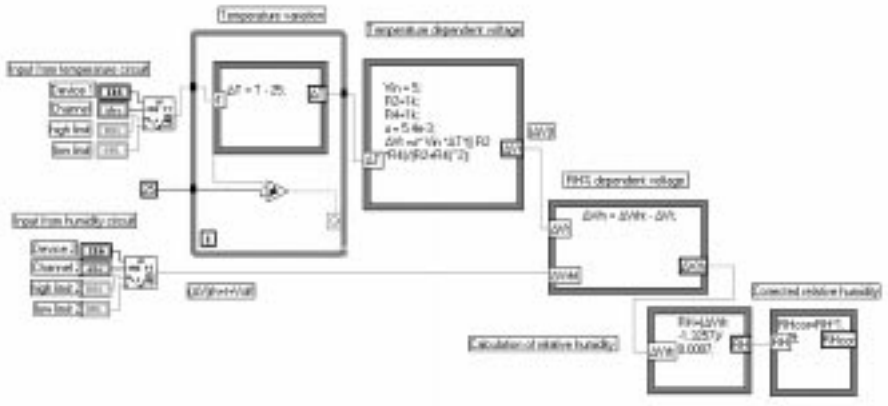

Fig. 8. Overview of error compensation system.

8 Conclusion

An adaptable, accurate humidity sensing system has been developed with full error compensation for a novel thin film resistive humidity sensor. The sensor is manufactured from a In_2O_3/SiO combination. The complete system has been designed and implemented using Lab-VIEW 6i. The interfering thermal effects and the bridge off-null conditions have been compensated for through the use of error-compensation algorithms. The main advantages of this system are the short development time, where a prototype can be produced rapidly, and the flexibility, where it can easily be modified to suit individual needs with little difficulty.

References

[1] P. R. Wiederhold: *Water Vapour Measurements: Methods and Instrumentation*, Marcel Dekker, Inc., 1997.
[2] M. Prudenziati: *Handbook of Sensors and Actuators* Vol. 1, Thick Film Sensors, Elsevier, 1994.
[3] G. Gusmano, G. Montesperelli, E. Traversa, A. Bearzotti: *Sens. Actuators*, B 14, pp. 525-527, 1993.
[4] W. Qu, W. Wlodarski: *Sens. Actuators*, B 64, pp. 42-48, 2000.
[5] Bowthorpe Thermistors, Crown Industrial Estate, Somerset TA2 8QY.
[6] C. D. Johnson: *Process Control Technology*, 6th Edition, Prentice Hall, 1999.
[7] J. H. Avery and A. W. K. Ingram: *Modern Laboratory Physics*, Heinemann Educational Books, Ch.6, 1971.